Journal of Alloys and Compounds, 203 (1994) 133–136
JALCOM 866

The crystal structure of $NdFe_{1-x}Sb_2$ and isotypic compounds $RE(Fe, Co)_{1-x}Sb_2$ (RE ≡ La, Ce, Pr, Sm, Gd)

A. Leithe-Jasper and P. Rogl*
Institut für Physikalische Chemie der Universität Wien, Währingerstraße 42, A-1090 Wien (Austria)

(Received June 15, 1993)

Abstract

New compounds $REFe_{1-x}Sb_2$ and $RECo_{1-x}Sb_2$ (RE ≡ La, Ce, Pr, Nd, Sm, Gd) were synthesized by argon arc melting elemental mixtures followed by annealing at 800 °C for 7 days. The crystal structure of $NdFe_{1-x}Sb_2$ was determined from single-crystal X-ray counter data. $NdFe_{1-x}Sb_2$ crystallizes in the $ZrCuSi_2$-type structure with the centrosymmetric space group *P4/nmm*. The tetragonal lattice parameters are $a = 0.43514(6)$ nm and $c = 0.96518(13)$ nm; $Z = 2$. For 273 reflections ($|F_o| > 2\sigma$) the residual values are $R_F = \Sigma|\Delta F|/\Sigma|F_o| = 0.0532$ and $R_w = 0.0516$. Compounds with the light rare earth elements La, Ce, Pr, Sm and Gd were found to be isotypic with $NdFe_{1-x}Sb_2$.

1. Introduction

In the course of a systematic search for novel permanent magnets in the Nd–Fe–Sb system [1], a hitherto unknown compound $NdFe_{1-x}Sb_2$ has been observed whose X-ray powder pattern is closely related to that of its homologue $CeNiSb_2$ [2]. The detailed investigation of the crystal structure of the novel compound and a systematic search for isotypic compounds within the series $REFe_{1-x}Sb_2$ and $RECo_{1-x}Sb_2$ (RE, rare earth) became the subject of the present work.

2. Experimental details

The alloys, each with a total weight of 1 g, were synthesized by argon arc melting from ingots of the elements, starting from nominal compositions (at.%) 30RE–13Fe–57Sb, 30RE–15(Fe, Co)–55Sb and 25RE–25Co–50Sb according to the homogeneity range and the Fe vacancies which were observed in the Nd–Fe–Sb system. The materials used were commercially available as high purity elements: rare earths were in the form of ingots (99.9% pure, Auer–Remy G.m.b.H., Germany); lumps of iron and cobalt (99.9% pure) were supplied by Johnson–Matthey & Co., UK; Sb was obtained as a rod (99.9% pure) from Johnson–Matthey & Co., UK.

To ensure homogeneity, the samples were remelted several times under an electric current as low as possible to minimize weight losses by vaporization of Sb, which were compensated beforehand by extra amounts of Sb. The approximate loss of Sb during the melting was 7 mass% of the nominal Sb composition. In order to avoid reaction of Sb with the Mo foil, which is usually used to protect the ingots in the annealing process from contamination by the hot quartz walls, the samples were placed in alumina crucibles, sealed in evacuated quartz tubes and annealed for 7 days at 800 °C. After the heat treatment the alloys were quenched by submerging the silica tubes in water.

Lattice parameters and standard deviations were determined by a least-squares refinement of room temperature 114.59 mm Debye–Scherrer X-ray powder data obtained using CrKα radiation. Owing to the sensitivity of the samples to moisture, the powders were protected in sealed glass capillaries during X-ray exposure.

3. Results and discussion

3.1. Structure determination

A rather small but isodimensional single-crystal fragment (about $40 \times 50 \times 60$ μm^3) was obtained by mechanical fragmentation of the well-crystallized solidified regulus of an alloy with the nominal composition (at.%) 15Nd–15Fe–70Sb which was annealed for 2 weeks at 850 °C in an evacuated quartz capsule.

*Author to whom correspondence should be addressed.

SSDI 0925-8388(93)00866-W

TABLE 1. Crystallographic data for $NdFe_{1-x}Sb_2$. Space group: $P4/nmm$–D_{4h}^7, No. 129, $Z=2$; origin at $\bar{1}$; $a=0.43514(6)$ nm, $c=0.96518(13)$ nm, $c/a=2.218$, $V=0.1827(1)$ nm^3, $\rho_x=8.06$ Mg m^{-3}

Atom	Site	x	y	z	Occupation	U_{11} (nm^2)	U_{22} (nm^2)	U_{33} (nm^2)
Nd1	2c	$\frac{1}{4}$	$\frac{1}{4}$	0.7580(1)	1.0	1.72(3)	1.72(3)	0.75(5)
Fe1	2a	$\frac{3}{4}$	$\frac{1}{4}$	0	0.6	2.68(16)	2.68(16)	1.16(22)
Sb1	2b	$\frac{3}{4}$	$\frac{1}{4}$	$\frac{1}{2}$	1.0	1.79(4)	1.79(4)	0.68(5)
Sb2	2c	$\frac{1}{4}$	$\frac{1}{4}$	0.1265(1)	1.0	2.27(4)	2.27(4)	1.93(7)

Anisotropic thermal factors are expressed as $T=\exp[-2\pi(U_{11}h^2a^{*2}+U_{22}k^2b^{*2}+U_{33}l^2c^{*2}+2U_{12}hka^*b^*+2U_{13}hla^*c^*+2U_{23}klb^*c^*)]\times10^{-2}$; by symmetry, $U_{12}=U_{13}=U_{23}=0$. Standard deviations are given in parentheses. The isotropic extinction parameter (SHELX-76) was $x=0.012$. The weighting scheme (SHELX-76) employed was $w(F)=8.1/[\sigma^2(F)+10^{-4}F^2]$. Residual values: $R_F=0.053$, $R_w=0.051$.

TABLE 2. Interatomic distances (nanometers) in $NdFe_{1-x}Sb_2$ up to 0.4 nm

Nd1–4Fe1	0.3192(1)	Fe1–4Sb2	0.2495(1)
4Sb2	0.3273(1)	(4Fe1	0.3077(0))
4Sb1	0.3307(1)	4Nd1	0.3192(1)
Sb2–4Fe1	0.2495(1)	Sb1–4Sb1	0.3077(0)
4Nd1	0.3273(1)	4Nd1	0.3307(1)

X-ray intensity data were collected on an automatic Stoe four-circle diffractometer for the full sphere of the reciprocal space out to a limit of $(\sin\theta)/\lambda=8.1$ nm^{-1} using monochromated Mo Kα radiation. A set of 278 symmetry-independent reflections was obtained by averaging symmetry-equivalent reflections out of a total number of 2743 recorded intensities; all observed intensities (273 for $|F_o|>2\sigma(F_o)$) were used in the structure refinement. An empirical absorption correction was applied using ψ scans of three independent reflections.

Laue and Weissenberg photographs taken along the [100] axis revealed tetragonal high Laue symmetry without any long-range order superstructure reflections; however, weak streaking effects (unsuitable for refinement) indicate a strong tendency towards supercell formation according to $a'\approx6a_0$ and $c'=3c_0$. Thus the only observed systematic extinctions were those of the n glide plane, $(hk0)$ for $h+k=2n+1$, altogether compatible with $P4/nmm$ as the centrosymmetric space group with the highest symmetry. Since the lattice parameters and X-ray powder intensities of the novel $REFe_{1-x}Sb_2$ phase revealed striking similarities to those of the homologous $CeNiSb_2$ [2], a first structure model was assigned for Nd, Fe and Sb atoms in the crystallographic positions of the $ZrCuSi_2$-type structure [3, 4]. This structure model was satisfactorily refined by employing the SHELX-76 program system [5]. The weights used were $w_i=8.1/[\sigma^2(F)+10^{-4}F^2]$ and structure factors with different weighting schemes had no significant influence on the atomic parameters obtained. Refinement of the Fe and Sb occupancies immediately revealed a significant deviation from full occupation of Fe at 2a sites but no indication of Sb deficiency. The final R values calculated for the anisotropic thermal parameters were $R_F=0.053$ and $R_w=0.051$. At this stage the final electron density map was featureless, confirming the composition $NdFe_{0.6}Sb_2$. Positional and thermal parameters are listed in Table 1; interatomic distances are given in Table 2. (A listing of F_o and F_c data is available on request.)

3.2. *Isotypic compounds*

Room temperature X-ray powder patterns of samples of $REFe_{1-x}Sb_2$ and $RECo_{1-x}Sb_2$ which had been annealed at 800 °C for 7 days revealed a convincing resemblance to the pattern of homologous $NdFe_{0.6}Sb_2$ and were all completely indexed on the basis of a tetragonal unit cell (see Table 3). Employing the atomic parameters derived for $NdFe_{1-x}Sb_2$ (Table 1), excellent agreement is obtained between the experimentally observed and calculated X-ray powder intensities, confirming the isotypy with the crystal structure of $ZrCuSi_2$. Furthermore, the homogeneity and X-ray intensities indicate an Fe deficiency in correspondence with the non-stoichiometric ratio RE/Fe(Co) in the nominal composition of the alloys.

Formation of the $REFe_{1-x}Sb_2$ and $RECo_{1-x}Sb_2$ series of compounds seems to be confined to the light rare earth metals. The stability appears to become reduced with decreasing radius of the rare earth element and $GdFe_{1-x}Sb_2$ is the smallest end member observed. No $RE(Fe, Co)_{1-x}Sb_2$ phase was found with the smaller rare earth metals Er, Dy and Y. The plot of the unit cell dimensions of the isostructural phases $REFe_{1-x}Sb_2$ and $RECo_{1-x}Sb_2$ in Fig. 1 merely reflects the lanthanoid contraction. There is no particular deviation from the general trends for the cerium-containing compounds, inferring a magnetically tripositive $^2F_{5/2}$ ground state for the Ce atoms.

TABLE 3. Crystallographic data for the compounds $RE(Fe, Co)_{1-x}Sb_2$ (RE ≡ La, Ce, Pr, Nd, Sm, Gd)

Nominal alloy composition (at.%)	Dimensions of unit cell (nm)		V (nm^3)	c/a
	a	c		
$La_{31}Fe_{14}Sb_{55}$	0.44035(7)	1.00113(22)	0.19425(7)	2.2735
$La_{30}Fe_{13}Sb_{57}$	0.44028(8)	1.00119(25)	0.19407(8)	2.2740
$Ce_{28}Fe_{17}Sb_{55}$	0.43768(6)	0.98271(22)	0.18824(6)	2.2453
$Ce_{30}Fe_{13}Sb_{57}$	0.43751(13)	0.98218(31)	0.11800(12)	2.2449
$Pr_{30.5}Fe_{14.5}Sb_{55}$	0.43616(10)	0.97552(29)	0.18558(10)	2.2366
$Pr_{30}Fe_{13}Sb_{57}$	0.43638(8)	0.97390(29)	0.18545(9)	2.2318
$Nd_{32}Fe_{13}Sb_{55}$	0.43479(9)	0.96554(20)	0.18253(8)	2.2207
$Nd_{31}Fe_{14}Sb_{57}$	0.43457(10)	0.96405(24)	0.18206(9)	2.2184
$Sm_{31}Fe_{13}Sb_{55}$	0.43261(8)	0.95156(12)	0.17808(6)	2.1996
$Sm_{30}Fe_{13}Sb_{57}$	0.43252(11)	0.95025(20)	0.17776(9)	2.1970
$Gd_{35}Fe_{10}Sb_{55}$	0.43080(7)	0.94125(19)	0.17469(6)	2.1849
$La_{30}Co_{15}Sb_{55}$	0.43854(6)	0.99232(23)	0.19084(7)	2.2628
$Ce_{25}Co_{25}Sb_{50}$	0.43747(7)	0.98214(24)	0.18796(7)	2.2450
$Ce_{30}Co_{15}Sb_{55}$	0.43588(9)	0.97479(30)	0.18521(9)	2.2364
$Pr_{28}Co_{17}Sb_{55}$	0.43415(11)	0.96700(26)	0.18243(10)	2.2294
$Nd_{25}Co_{25}Sb_{50}$	0.43453(10)	0.96918(30)	0.18300(10)	2.2304
$Nd_{30}Co_{15}Sb_{55}$	0.43306(7)	0.96138(24)	0.18029(8)	2.2200
$Sm_{28}Co_{17}Sb_{55}$	0.43415(11)	0.96700(26)	0.18243(10)	2.2294

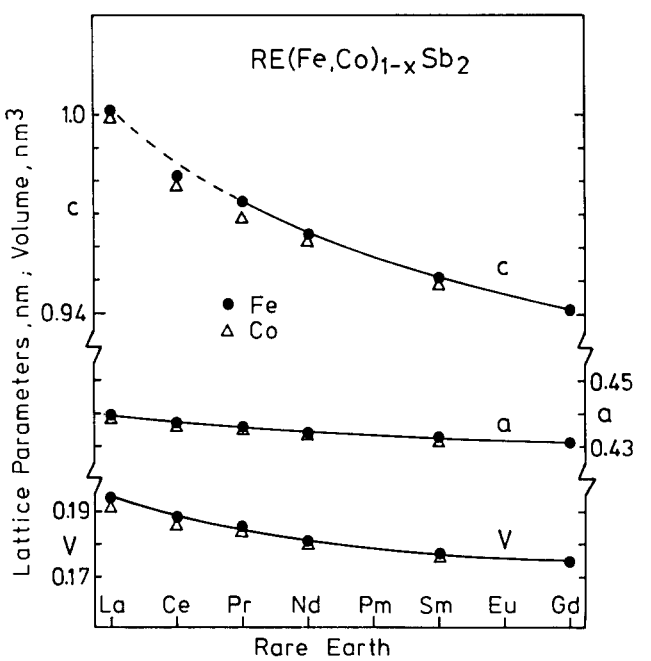

Fig. 1. Lattice parameters and volumes of the compounds $REFe_{1-x}Sb_2$ and $RECo_{1-x}Sb_2$ *vs.* the rare earths. Data refer to the (Fe, Co)-poor phase boundary.

3.3. Crystal chemistry

Figure 2 is a representation of the crystal structure of $NdFe_{1-x}Sb_2$ in three-dimensional view. Some confusion exists about the prototype of compounds such as $NdFe_{1-x}Sb_2$. The site occupation and atomic parameters are compatible with the crystal structure of

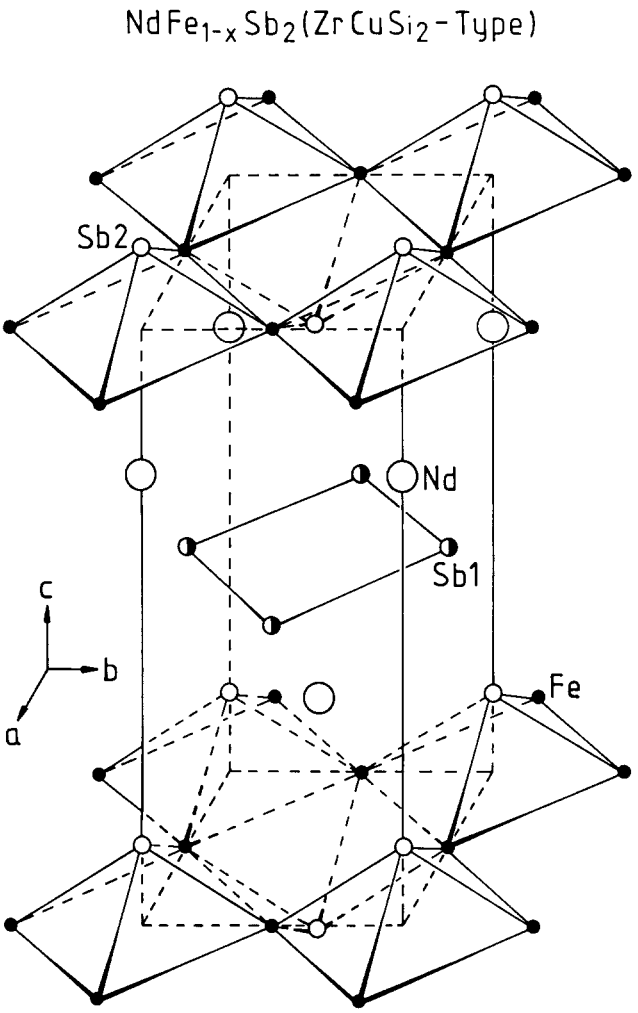

Fig. 2. Crystal structure of $NdFe_{1-x}Sb_2$ in three-dimensional view (centre at (½ ½ 0) of unit cell).

$CaMnBi_2$ [6], which has been described as a unique structure type by Cordier *et al.* [7] but has been listed by Villars and Calvert [8] as a representative of the ZrCuSiAs type. The crystal structure of $ZrCuSi_2$ [3, 4] and in particular the ordered derivative ZrCuSiAs [9] in turn have earlier been regarded as a filled version of the PbFCl or Cu_2Sb type [9] or as an intercalation of planar copper atom layers in the $ZrSi_2$-type structure [4] (see Fig. 2). Following the interpretation of $CaMnBi_2$ by Parthé and Chabot [10], $NdFe_{1-x}Sb_2$ is preferably considered as an intergrowth structure combining slabs of the $BaAl_4$ type, as seen in $Ce(Ni, Sb)_4$ [2], with slabs of the $ZrSi_2$ type. The latter description refers to the formation of tetrahedra consisting of the metametal component atoms (Sb2) centred by the small transition metal atoms (Fe1). The interatomic distances Fe1–Sb2 are extremely short (see Table 2) compared with the sum of the metal radii, thereby suggesting strong transition metal–metametal bonding as well as providing a satisfactory explanation of the observed Fe deficiency which eventually results in the formation of

supercells as a function of particular ordering among Fe atoms and vacancies. The distances between the iron atoms are rather large (0.3077 nm), reflecting weak bonding in correspondence with weak magnetic interaction.

Acknowledgments

The research reported herein has been sponsored by the Austrian Science Foundation (FFWF Project No. P8218). We also wish to acknowledge a grant from the Austrian National Bank (Project No. 3804).

References

1 A. Leithe-Jasper, *Thesis,* University of Vienna, 1993, pp. 1–86.
2 Yu.V. Pankevich, V.K. Pecharskiy and O.I. Bodak, *Metally, 5* (1983) 227–229.
3 H. Sprenger, *J. Less-Common Met., 34* (1974) 39.
4 F. Thirion, G. Venturini, B. Malaman, J. Steinmetz and B. Roques, *J. Less-Common Met., 95* (1983) 47–54.
5 G. Sheldrick, *SHELX, Program for Crystal Structure Determination,* University of Cambridge, 1976.
6 E. Brechtel, G. Cordier and H. Schäfer, *Z. Naturf. B, 35* (1980) 1–3.
7 G. Cordier, H. Schäfer and P. Woll, *Z. Naturf. B, 40* (1985) 1097–1099.
8 P. Villars and L.D. Calvert, in *Pearson's Handbook of Crystallographic Data for Intermetallic Phases,* ASM, Materials Park, OH, 2nd edn., 1991.
9 V. Johnson and W. Jeitschko, *J. Solid State Chem., 11* (1974) 161–166.
10 E. Parthé and B. Chabot, in K.A. Gschneidner and L. Eyring (eds.), *Handbook on the Physics and Chemistry of the Rare Earths,* Vol. 6, North-Holland, Amsterdam, 1984, p. 113.